npj | biofilms and microbiomes

Article

Published in partnership with Nanyang Technological University

https://doi.org/10.1038/s41522-025-00706-w

Targeted metabolomics reveals bioactive inflammatory mediators from gut into blood circulation in children with NAFLD

Miyang Luo[1], Jiayou Luo[1], Atipatsa C. Kaminga[1], Jia Wei[1], Wen Dai[1], Yan Zhong[2], Ningan Xu[2], Xiongwei Li[3], Haixiang Zhou[3] & Xiongfeng Pan[4,5] ✉

Altered gut metabolites are important for the inflammatory progression in children with NAFLD. Fecal and plasma samples were collected from 145 subjects including 53 non-alcoholic fatty liver (NAFL), 39 nonalcoholic steatohepatitis (NASH) and 53 obese controls. We performed G350 targeted integrative metabolomics using high performance liquid chromatography mass spectrometry for fecal and plasma analysis of NAFL, NASH, and obese children. We found 9 metabolites involved in metabolic reprogramming of inflammation in NAFLD, such as lipid, carbohydrate, amino acid metabolism, and TCA cycle pathway. Moreover, 7 inflammation-related metabolites could discriminate NAFLD severity by machine learning model. This study identified three novel elevated inflammatory pathogenic metabolites and the relationship between increased inflammation, may be involved in TLR5/MYD88/NFκB pathway. These findings reveal that specific inflammatory metabolites entering the blood circulation from the gut are associated with disease severity and inflammatory pathogenesis in children with NAFLD.

Non-alcoholic fatty liver disease (NAFLD) is the leading cause of chronic liver disease worldwide in childhood[1,2]. Children with non-alcoholic fatty liver simple steatosis (NAFL) may develop nonalcoholic steatohepatitis (NASH), which is characterized by hepatic inflammation and cell injury, and increases the risk of hepatocellular carcinoma in adulthood[3]. The pathogenesis of NAFLD is poorly characterized, emerging evidence suggests that the gut microbiome influences the severity and inflammatory progression of NAFLD[4,5].

Although some studies have demonstrated that the microbiota influence on inflammatory progression by gut metabolites, and identified some inflammatory gut metabolites for NAFLD, such as ursodeoxycholic acid, arachidonic acid, phenylacetic acid, branched-chain amino acids, and indolic[6–11]. However, in view of the diversity and magnitude of the gut metabolites network, there are many unknown metabolites that have not been explored. Identifying inflammatory gut metabolites using low through-put targeted analyses is limited to a certain class of metabolites, and cannot systematically explore the phenotypes of gut metabolite profiles. The identification and validation of inflammatory gut metabolites in gut-liver axis requires "high-throughput omics" approach, such as fatty acids, amino acids, bile acids, benzenoids, carbohydrates, indoles, and purine nucleotides. It is also noteworthy that the gut metabolites species from gut into blood circulation in children with NAFLD are still not fully understood. Furthermore, specific significant gut metabolite pathways that may be involved in the inflammatory progression of NAFLD remain unexplored.

The aims of this study were as follows: (i) to perform a "G350 high-throughput omics" approach to reveal potential metabolic alterations in feces and plasma of children with NAFLD; (ii) to reveal potential metabolic alterations from the gut into blood circulation, then evaluate the potential inflammatory pathogenesis pathways and inflammatory changes related to these metabolites; and (iii) to apply multiple validations of the inflammatory effect for these metabolites, such as machine learning and in vitro cell experiment. The findings of this study would provide insights into the gut-liver axis, evaluation of potential inflammatory pathogenesis, and the search for immunotherapeutic biomarkers for children with NAFLD.

Results

Participant characteristics

The baseline demographics and laboratory parameters are shown in Supplementary Table 1 and Supplementary Table 2. According to the

[1]Department of Epidemiology and Health Statistics, Department of Maternal and Child Health, Xiangya School of Public Health, Central South University, Changsha, China. [2]Institute of Children Health, Hunan Children's Hospital, Changsha, Hunan, China. [3]Center for Disease Control and Prevention of Ningxiang, Changsha, Hunan, China. [4]Pediatrics Research Institute of Hunan Province, Hunan Children's Hospital, The Affiliated Children's Hospital of Xiangya School of Medicine, Central South University, Changsha, China. [5]The Affiliated Children's Hospital of Xiangya School of Medicine, Central South University, Hunan Provincial Key Laboratory of Pediatric Orthopedics, The school of pediatrics, University of South China, Hengyang, Hunan, China. ✉e-mail: pxfcsu@163.com

distribution of characteristics data, there was good comparability between the case and control groups.

Distinct distribution of gut metabolites in children with NAFLD and control in fecal samples

The principal components analysis of fecal (Supplementary Fig. 1a) and plasma (Supplementary Fig. 1b) results shown that QC samples are closely gathered, indicating that the data quality was stable and accurate. The TIC plots showing the results of the differential fecal and plasma metabolites on Amide column and C18 columns (Supplementary Fig. 2). A total of 266 annotated metabolites were detected in fecal samples (Fig. 1A). Distinct clusters of gut metabolites were demonstrated in fecal samples (R2Y = 0.802 and Q2Y = 0.841) in children with NAFL compared with control children by OPLS-DA score plots (Fig. 1B). Significant differences were also found for the following groups: NASH children compared with control children (R2Y = 0.742 and Q2Y = 0.834); and NASH children compared with NAFL children (R2Y = 0.659 and Q2Y = 0.698). Moreover, the intercepts for goodness-of-prediction (Q2) and goodness-of-fit (R2) indicated that the OPLS-DA model containing metabolomics information was reliable and not overfitting (Fig. 1C).

The volcano plots showed that 16 metabolites were significantly increased and 12 metabolites were significantly decreased in the NAFL group compared with the control children, whereas 62 metabolites were significantly increased and 17 metabolites were significantly decreased in the NASH children compared with the control children. Compared with the NAFL children, 34 metabolites were significantly increased and 12 metabolites were significantly decreased in the NASH children (Fig. 1D).

Distinct distribution of gut metabolites in children with NAFLD and control in plasma samples

A total of 212 annotated metabolites were detected in plasma samples (Fig. 2A). Distinct clusters of gut metabolites in NAFL children compared with control children were demonstrated in plasma samples (R2Y = 0.629 and Q2Y = 0.871) by OPLS-DA score plots (Fig. 2B). Significant differences were also found for the following groups: NASH children compared with control children (R2Y = 0.609 and Q2Y = 0.923); and NASH children compared with NAFL children (R2Y = 0.639 and Q2Y = 0.886). Furthermore, the intercepts of goodness-of-prediction (Q2) and goodness-of-fit (R2) indicated that the OPLS-DA model containing metabolomics information was reliable and not overfitting (Fig. 2C).

The volcano plots showed that 33 metabolites were significantly increased and 32 metabolites were significantly decreased in the NAFL group compared with the control children, whereas 52 metabolites were significantly increased and 41 metabolites were significantly decreased in the NASH children compared with the control children. Compared to the NAFL children, 38 metabolites were significantly increased and 31 metabolites were significantly decreased in the NASH children (Fig. 2D).

Identification of signature metabolites for NAFLD from gut into blood circulation

We further selected the differential inflammation-related metabolites in the correlation analysis as independent variables, and established a machine learning model to distinguish different states of NAFLD. The metabolite, 2-Hydroxy-3-methylbutyric acid, could distinguish, using machine learning, NAFL children from the controls in feces and plasma. Also, the 2-Hydroxy-3-methylbutyric acid was significantly correlated with markers of glycolipid metabolism, and liver function. Furthermore, the three metabolites, namely 2-Hydroxy-3-methylbutyric acid, L-Thyronine, and L-Alanine could distinguish NASH children from the NAFL children by machine learning in feces and plasma. These metabolites were also significantly correlated with markers of inflammation, gut microbiota, glycolipid metabolism, and liver function. The six metabolites, 2-Hydroxy-3-methylbutyric acid, Indole, L-Thyronine, w-TMCA, cis-Aconitic acid and Ribonolactone could also distinguish NASH children from the controls by machine learning in feces and plasma (Supplementary Table 3).

The key metabolic pathways in the inflammatory pathogenesis of NAFLD

We further utilized the differential metabolites for pathway enrichment analysis and functional annotation to find the metabolic pathways related to inflammation. Pathway analysis of these different gut metabolites between children with NAFL and controls revealed that several processes were significantly enriched. Pathway analysis identified significant differences in amino acid metabolism, carbohydrate metabolism, digestive system, and energy metabolism as the most enriched pathways in fecal and plasma samples (Fig. 3A, B and Supplementary Table 4). These different gut metabolites, between NASH children and controls, are involved in several processes, such as amino acid metabolism, carbohydrate metabolism, digestive system, energy metabolism and metabolism of cofactors and vitamins; and were the most enriched pathways in fecal and plasma samples (Fig. 3A, B and Supplementary Table 5). We compared the metabolomic profiling of NAFL to the NASH to identify metabolic pathways involved in the progression of NASH. We identified significant differences in amino acid metabolism, digestive system, and metabolism of cofactors, with vitamins being the most enriched pathways in fecal and plasma samples (Fig. 3A, B and Supplementary Table 6).

These metabolites were significantly changed in the cases, and were associated with impaired inflammation, gut microbiota, glycolipid metabolism, and liver function through critical metabolic pathways such as amino acid metabolism, carbohydrate metabolism, digestive system, energy metabolism and metabolism of cofactors and vitamins. Metabolites associated with these metabolic pathways have been reported to contribute to the pathogenesis of systemic gut inflammation and liver inflammation in NAFLD patients (Fig. 3C and Table 1). After adjusting the major confounding factors such as age, gender and BMI, we found that metabolites such as 2-Hydroxy-3-methylbutyric acid, Indole-3-lactic Acid, 2-Furoic acid, cis-Aconitic acid, and L-Isoleucine in plasma may be risk factors for children with NAFLD, while L-Thyronine may be a protective factor for children with NAFLD (Supplementary Table 7).

The correlation between selected metabolites with NAFLD indices in plasma samples

Considering the 24 differential metabolites, all of them were significantly associated with at least one inflammatory factor, with 22 of them positively correlated with inflammatory factors. Specifically, 6 metabolites (Beta-Alanine, cis-Aconitic-acid, L-Alanine, L-Valine, Sarcosine, Alpha-ketoisovaleric-acid) had a positive correlation with the levels of 8 inflammatory factors; 5 metabolites (L-Alloisoleucine, L-Isoleucine, L-Leucine, L-Norleucine, and 2-Hydroxy-3-methylbutyric-acid) had a positive correlation with the levels of 7 inflammatory factors; 2 metabolites (L-Homoserine and L-Phenylalanine) had a positive correlation with the levels of 6 inflammatory factors; w-TMCA had a positive correlation with the levels of 5 inflammatory factors; 4 metabolites (Indole-3-lactic-Acid, N-acetyltryptophan, w-MCA, and 2-Furoic-acid) had a positive correlation with the levels of 4 inflammatory factors; ribonolactone had a positive correlation with the levels of 3 inflammatory factors; 2 metabolites (a-TMCA and b-TMCA) had a positive correlation with the levels of 2 inflammatory factors; arachidonic acid had a positive correlation with the level of 1 inflammatory factor; whereas indole had a negative correlation with the levels of 8 inflammatory factors; and L-Thyronine had a negative correlation with the levels of 5 inflammatory factors. Moreover, we compared these selected significant metabolites in plasma samples with gut microbiota, glycolipid metabolism, and liver function (Supplementary Table 8 and Fig. 4A).

qRT-PCR verification of differentially expressed mRNAs of liver function and inflammation

The mRNA relative expression levels of ALT, CXCL8, IL6, IL17, IL21 and TNFα genes in THLE-3 were significantly upregulated after exposure to 2-Hydroxy-3-methylbutyric acid. In terms of related receptors, the level of TLR5 gene relative expression was significantly increased. Moreover, the IL1β relative expression was significantly suppressed after exposure to

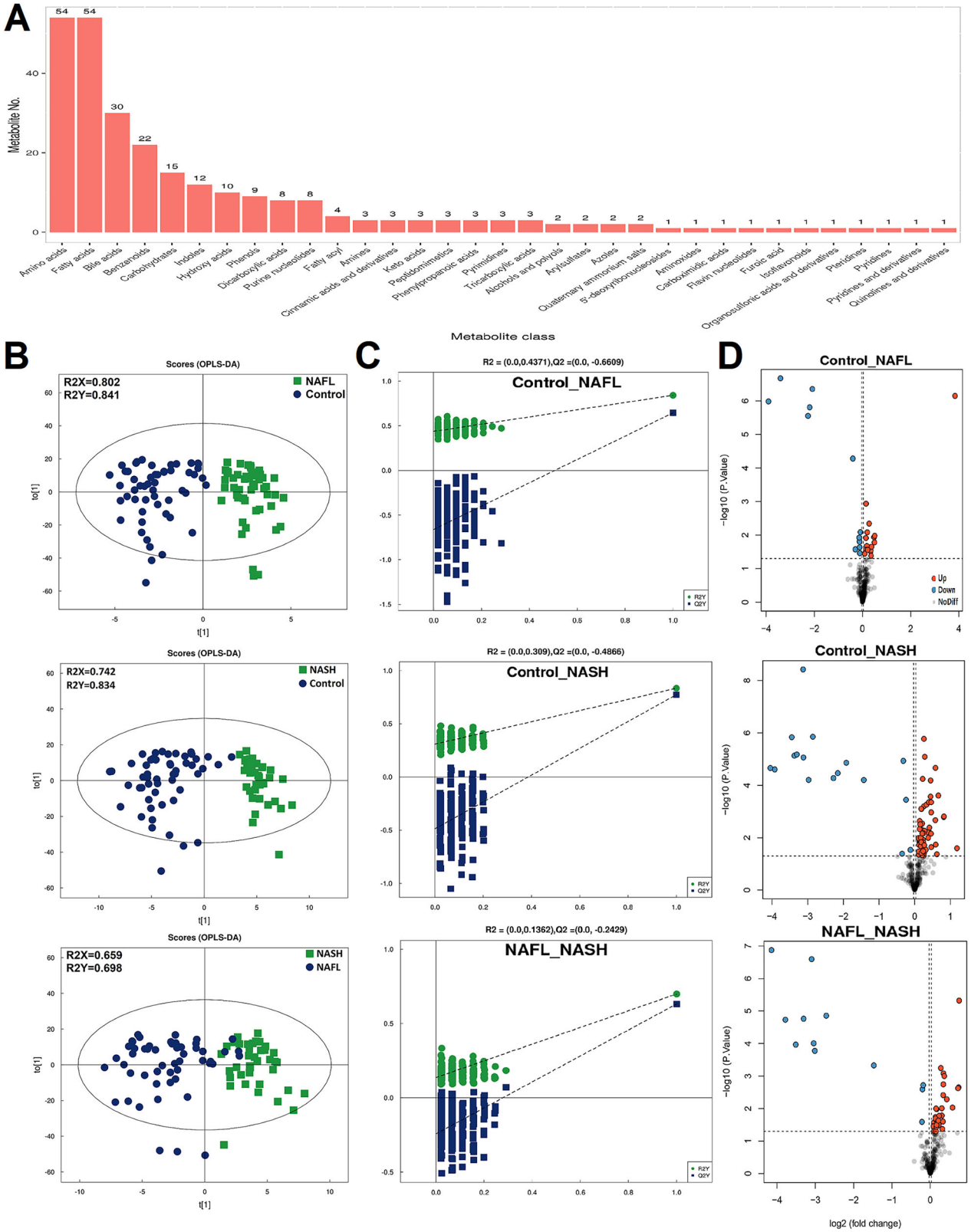

Fig. 1 | Gut metabolic alterations in NAFLD. Chemical class metabolite sets plots (**A**) shown the chemical class metabolite of metabolites. **B** OPLS-DA score plots for differential metabolites in fecal samples. X axis and Y axis represent contributions of persons to the first two principal components (PC1 and PC2). **C** Cross-validation plot with a permutation test repeated 200 times. The intercepts of R2 and Q2 suggest that the OPLS-DA model is not overfitting. **D** Volcano plots shown the results of pairwise comparisons of metabolites in each case sample's group relative to controls. The abscissa represents the variation of variation multiple of metabolites in different groups (log2 Fold Change), and the ordinate represents the significance level (−log10 p-value). The vertical dashed lines indicate the threshold for the abundance difference. The horizontal dashed line indicates the $p = 0.05$ threshold. Each point in the graph represents metabolites, the up-regulated metabolite red dot, the down regulated metabolite green dot. Between-group comparisons were performed using empirical Bayes hierarchical model and Kruskal-Wallis rank sum test. OPLS-DA Orthogonal Partial Least Squares Discrimination Analysis, NAFL nonalcoholic fatty liver, NASH non-alcoholic steatohepatitis.

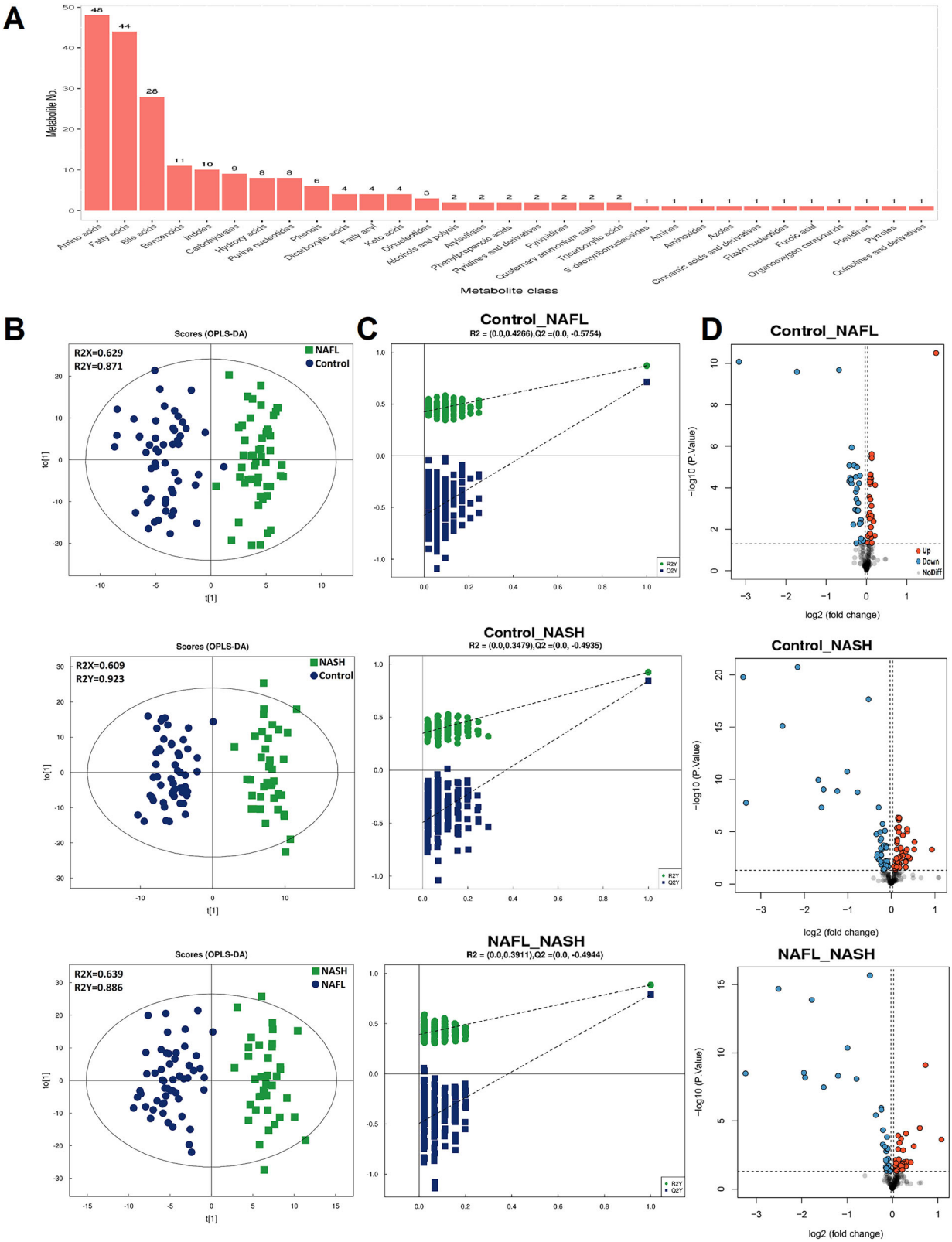

Fig. 2 | Plasma metabolic alterations in NAFLD. Chemical class metabolite sets plots (**A**) shown the chemical class metabolite of metabolites. **B** OPLS-DA score plots for differential metabolites in Plasma samples. X axis and Y axis represent contributions of persons to the first two principal components (PC1 and PC2). **C** Cross-validation plot with a permutation test repeated 200 times. The intercepts of R2 and Q2 suggest that the OPLS-DA model is not overfitting. **D** Volcano plots shown the results of pairwise comparisons of metabolites in each case sample's group relative to controls. The abscissa represents the variation of variation multiple of metabolites in different groups (log2 Fold Change), and the ordinate represents the significance level (−log10 p-value). The vertical dashed lines indicate the threshold for the abundance difference. The horizontal dashed line indicates the $p = 0.05$ threshold. Each point in the graph represents metabolites, the up-regulated metabolite red dot, the down regulated metabolite green dot. Between-group comparisons were performed using empirical Bayes hierarchical model and Kruskal-Wallis rank sum test. OPLS-DA Orthogonal Partial Least Squares Discrimination Analysis, NAFL nonalcoholic fatty liver, NASH non-alcoholic steatohepatitis.

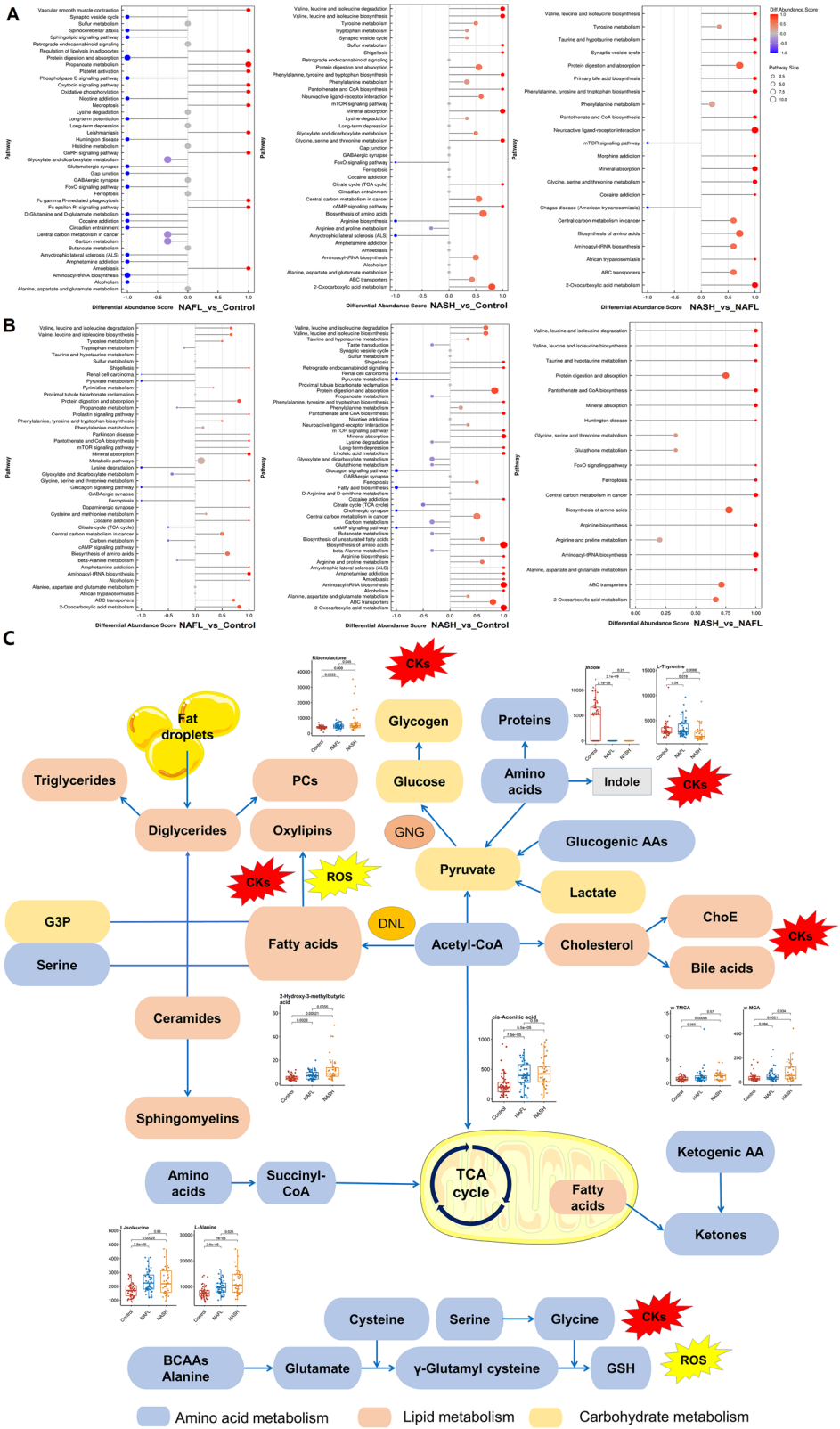

Fig. 3 | Overview of the key gut metabolic pathways in the pathogenesis of NAFLD. Pathway enrichment plots of fecal (**A**) and plasma (**B**) shown the pathway enrichment analysis by KEGG for metabolites. The pathway enrichment analysis result takes KEGG pathway as the unit, and the hypergeometric test is applied to find the pathway that is enriched in the differential metabolites against the background of all identified metabolites. Pathway enrichment analysis can determine the most important metabolic pathways and signal transduction pathways involved in the differential metabolites. An overview plot shown the key metabolic pathways in the pathogenesis of NAFLD (**C**). Boxplots show levels of these metabolites in the plasma samples at different stages. AAs amino acids, PCs Phosphatidylcholines, BCAAs branched-chain amino acids, ChoE cholesterol esters, CoA coenzyme A, G3P glyceraldehyde 3-phosphate, GNG gluconeogenesis, CKs Inflammatory cytokines, ROS reactive oxygen species, SFA saturated fatty acid, TCA tricarboxylic acid. NAFL nonalcoholic fatty liver, NASH non-alcoholic steatohepatitis.

Table 1 | Dysregulation of the significantly pathway of metabolites might be involved in the inflammatory progression of NAFLD

Metabolites	Carbohydrate metabolism	Lipid metabolism	Amino acid metabolism	Inflammatory pathway
2-Furoic acid				
2-Hydroxy-3-methylbutyric acid	*	*		☆
Alpha-ketoisovaleric acid				
Arachidonic acid				
Beta-Alanine		*	*	
Cis-Aconitic acid	*	*		☆
Indole	*			☆
Indole-3-lactic Acid		*		
L-Alanine		*	*	☆
L-Alloisoleucine			*	
L-Homoserine			*	
L-Isoleucine	*		*	☆
L-Leucine			*	
L-Norleucine			*	
L-Phenylalanine		*	*	
L-Thyronine			*	☆
L-Valine			*	
N-acetyltryptophan	*	*		
Omega-muricholic acid		*		☆
Ribonolactone	*			☆
Sarcosine		*	*	
Tauro-a-muricholic acid				
Tauro-b-muricholic acid	*			
Tauro-w-muricholic acid	*	*		☆

*significantly metabolism pathway of metabolites; ☆, metabolites involved in the inflammatory pathway.

Indole, the FXR relative expression was significantly increased. The relative expression level of IL-6 gene was significantly upregulated exposure to Ribonolactone, relative expression level of NFκB gene was significantly upregulated. The relative expression levels of IL-6 and IL-17 genes were significantly upregulated exposure to cis-Aconitic acid, MYD88, NFκB and TLR5 genes were also significantly upregulated (Fig. 4B). There was no significant difference in the expression level of inflammatory factor genes in THLE-3 after exposure to Tauro-w-muricholic acid, L-Thyronine and L-Alanine (Supplementary Fig. 3).

Molecular docking of metabolites to binding domain of inflammatory receptor protein

List of metabolites included in the molecular docking analysis were shown in Supplementary Table 9. The S value for the TLR5 binding cis-Aconitic acid and 2-Hydroxy-3-methylbutyric acid were −5.41 kcal/mol and −4.71 kcal/mol. The S value for the NFκB binding Ribonolactone and cis-Aconitic acid were −4.61 kcal/mol and −4.68 kcal/mol. The S value for the MyD88 binding cis-Aconitic acid was −5.39 kcal/mol. The S value for the FXR binding Indole was −4.68 kcal/mol (Supplementary Table 10). Many hydrophobic amino acid residues surrounded the metabolites (Fig. 5A, B). These data indicated that the binding pocket of inflammatory receptor protein is suitable for molecule interactions and metabolites may serve as a ligand specifically bound to this ligand-binding domain for modulation of inflammatory receptor activity. This study identified three inflammatory pathogenic metabolites (2-Hydroxy-3-methylbutyric acid, Ribonolactone, and cis-Aconitic acid), may be involved in TLR5/MYD88/NFκB pathway.

Discussion

For the first time in this study, we systematically performed an in-depth and comprehensive gut targeted metabolomic profiling of plasma and fecal samples to identify NAFLD-associated metabolites in children with obesity, NAFL, and NASH. Targeted metabolomics revealed extensive inflammatory mediators from gut into plasma in children with NAFLD. We found 22 significantly increased metabolites and 2 significantly decreased metabolites in fecal and plasma samples of the NAFL or NASH children than in the controls. Moreover, 9 metabolites (2-Hydroxy-3-methylbutyric acid, cis-Aconitic acid, w-TMCA, w-MCA, indole, Ribonolactone, L-Isoleucine, L-Alanine and L-Thyronine) were significantly correlated with inflammatory factors and associated with inflammatory metabolic pathways. These metabolites were also involved in amino acid metabolism, carbohydrate metabolism, digestive system, tricarboxylic acid (TCA) cycle, energy metabolism and metabolism of cofactors and vitamins. Regarding disease status, metabolite fingerprinting by machine learning revealed 7 metabolites (2-Hydroxy-3-methylbutyric acid, w-TMCA, indole, Ribonolactone, cis-Aconitic acid, L-Alanine and L-Thyronine) that discriminated different stage of NAFLD. Meanwhile, one of the advantages of our research was that targeted metabolomics, could be used for absolute quantification rather than relative quantification. Moreover, by analyzing the 24 differentially expressed metabolites screened by machine learning, we found that 95.8% of the metabolites had fecal concentrations higher than plasma concentrations, except for cis-Aconitic acid, which may be due to its involvement in energy metabolism leading to higher endogenous production concentrations than in fecal. Future animal experiments are needed to compare the concentrations of metabolites in the gut, liver and circulation to further determine whether they are produced by liver metabolism.

Although the inflammatory metabolite, indole, was previously reported in NAFLD, the following inflammatory metabolites in NAFLD are being reported for the first time: 2-Hydroxy-3-methylbutyric acid, L-Alanine, cis-Aconitic acid, Ribonolactone, L-Thyronine, and w-TMCA. Gut microbiota and metabolites have been considered to be key factors affecting hepatic lipid

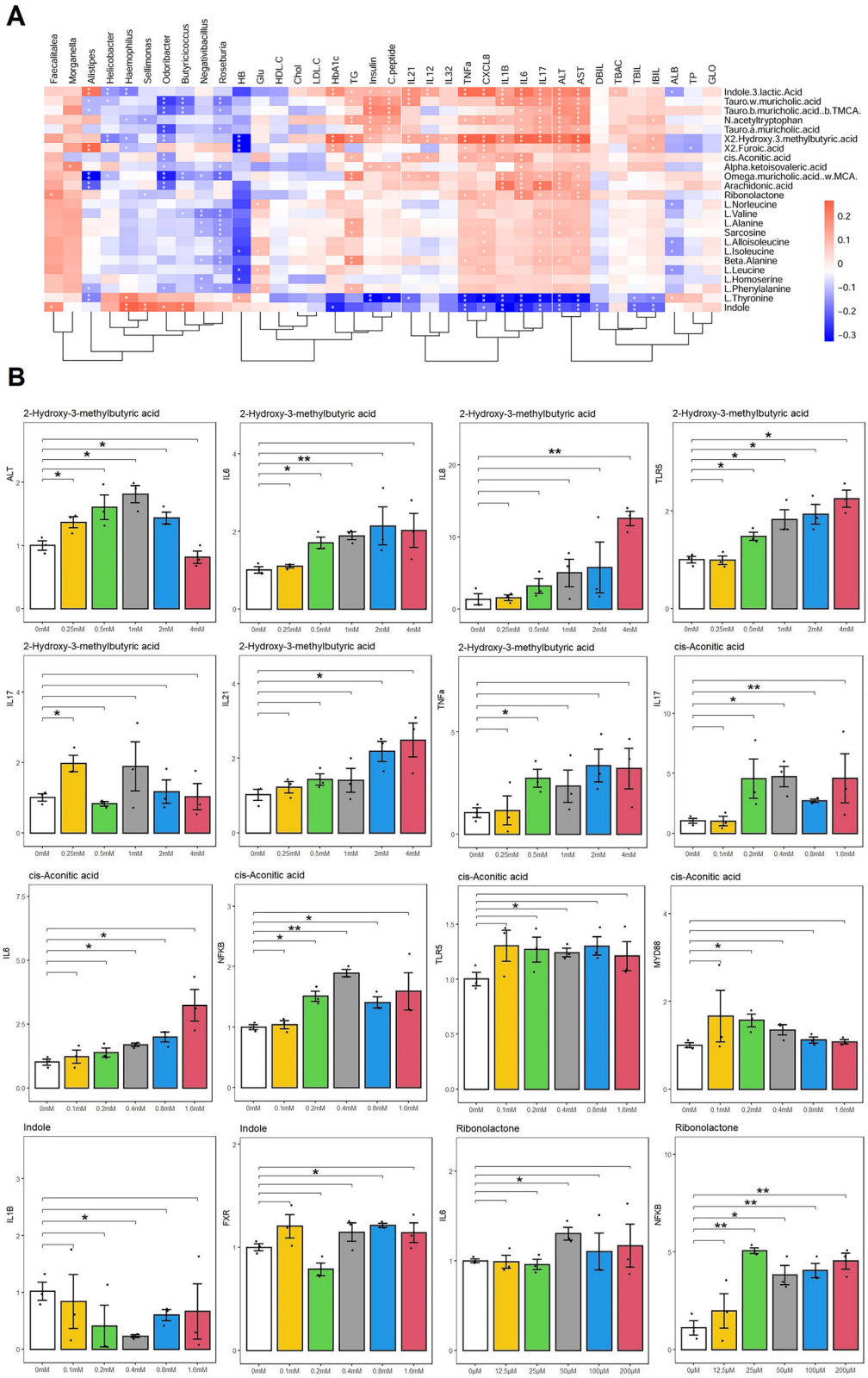

Fig. 4 | Metabolites discriminates disease severity and association of mediators with markers of inflammation, glycolipid metabolism and liver function. A heatmap of plasma (**A**) shown the correlation between selected gut metabolites with glycolipid metabolism, liver function and inflammatory factors indices. Red color represents positive correlation, blue color represents negative correlation. Bar chart (**B**) show the qRT-PCR of differentially relative expressed mRNAs of liver function and inflammation produced by THLE-3 under different treatments, C control group, NAFL nonalcoholic fatty liver, NASH non-alcoholic steatohepatitis. $p < 0.05$ was considered statistically significant. $^{*}p < 0.05$; $^{**}p < 0.01$.

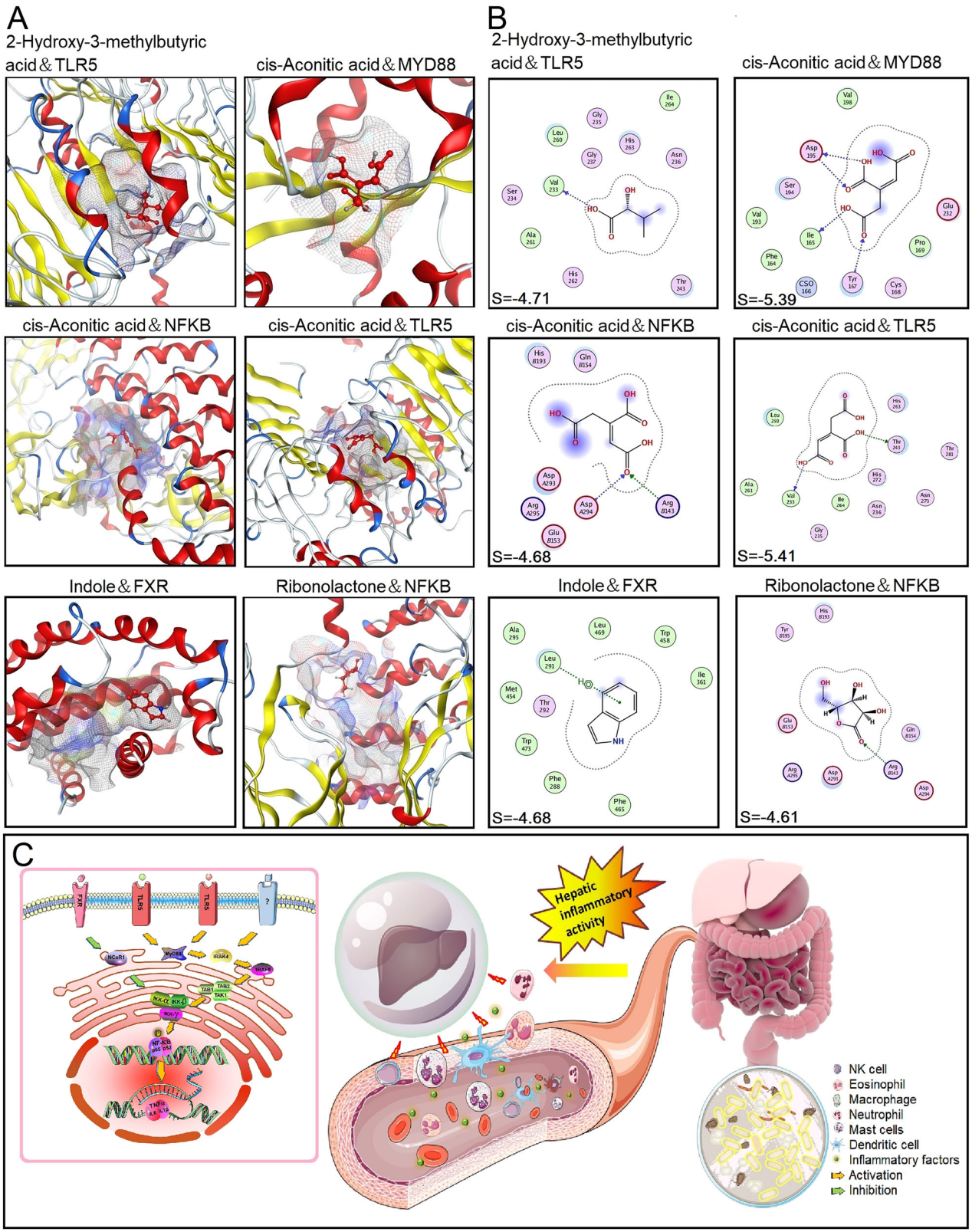

Fig. 5 | Metabolites docks to the ligand-binding domain of inflammatory receptor. The superposition of these metabolites bound to the ligand-binding domain pocket of inflammatory receptor (**A**). Two-dimensional interaction map of inflammatory receptor with metabolites (**B**). Hypothesis map of inflammatory mechanism pathway is shown in (**C**).

accumulation and inflammation during the development of liver diseases, such as NAFLD and hepatocellular carcinoma[12,13]. The following discussion focuses on how the metabolites, found by machine learning in this study, produce inflammatory effects through different metabolic pathways. Overall, these metabolites seem to form a TCA cycle metabolic network in amino acid, lipid, and carbohydrate metabolism. First, in amino acid metabolism, branched-chain amino acids are used to synthesize glutathione in response to oxidative stress and inflammation[14,15]. L-Thyronine seems to have similar

functions with branched-chain amino acids, which can inhibit inflammation. However, in this study, L-Alanine, L-Valine, Sarcosine and L-Isoleucine seem to have antagonistic effects with branched-chain amino acids. These amino acid metabolites may inhibit glutathione production and activate inflammatory response. Second, in lipid metabolism, liver steatosis is an important part of NAFL and NASH, which is mainly caused by the imbalance of triglyceride production and secretion in the liver[16]. Hepatic de novo lipogenesis is stimulated by carbohydrate and insulin, and the metabolism of fatty acids produces oxylipins, which usually increase the risk of inflammatory-related diseases such as insulin resistance, diabetes, and obesity[17,18]. In this study, Hydroxy-3-methylbutyric acid, a lipid metabolite, may be involved in the metabolism of fatty acids and oxylipins, thus promoting inflammation and NASH. Bile acids are secreted in response to the meal to facilitate the digestion of fats[19]. Disturbance of bile acid metabolism leads to underactivation of bile acid receptors FXR and TGR5, causal for decreased energy expenditure, increased lipogenesis, bile acid synthesis and hepatic inflammation[20]. This phenomenon was also observed in this study. The levels of bile acid metabolites w-MCA and w-TMCA were significantly increased in NASH group, which may promote the occurrence and development of inflammation and NASH. Finally, in carbohydrate metabolism, excessive hepatic mitochondrial TCA cycle and gluconeogenesis in patients with NAFLD[21,22]. In this study, Ribonolactone, a metabolite of carbohydrates, and cis-Aconitic acid, an intermediate of TCA cycle, may participate in the energy metabolism in the occurrence and development of NASH, and may promote inflammation. These findings raise the possibility that dysregulated TCA cycle metabolism is central in the NAFLD, providing a potential link between amino acid, lipid, and carbohydrate metabolism.

Specifically, among these inflammatory mediators, 2-Hydroxy-3-methylbutyric acid belongs to the class of hydroxy fatty acids and is mainly involved in lipid metabolism pathways. The 2-Hydroxy-3-methylbutyric acid showed good ability to distinguish NAFL/NASH from controls in a machine learning model, and it has been identified in the urine of patients with maple syrup urine disease and lactic acidosis[23,24]. In another study, altered 2-Hydroxy-3-methylbutyric acid was correlated with severity of inflammation, which has important diagnostic value for community-acquired pneumonia[25]. These findings are particularly consistent with our finding that the level of 2-Hydroxy-3-methylbutyric acid was significantly upregulated in NAFLD patients, and associated with impaired inflammation (IL1β, IL6, IL17, IL21, IL32, TNFα, and CXCL8), glycolipid metabolism, and liver function.

Lipid metabolism in the liver is mainly involved in the occurrence and development of NAFLD through two metabolic pathways, one of which is oxidized to produce energy and ketones, such as acetoacetate and β-hydroxybutyric acid[26]. The other metabolic pathway is re-esterified to glycerol esters, such as diglycerides and triglycerides. Primary bile acids and cholesterol esters are synthesized from cholesterol. Bile acid metabolism is involved in the progression of NAFLD's response to a high-fat diet to facilitate the digestion of fats[27,28]. Glyceraldehyde 3-phosphate, serine and diglycerides are also involved in the synthesis of sphingomyelins and ceramides[29,30]. Newly synthesized triglycerides can be secreted as VLDL or stored as lipid droplets. These metabolic pathways have the effect of promoting liver inflammation and oxidative stress[4].

Cis-Aconitic acid belongs to the class of tricarboxylic acids (TCA) and derivatives, and is mainly involved in the TCA cycle pathway. In a machine learning model, cis-Aconitic acid showed good ability in the discrimination of the NASH patients from the controls. Also, cis-Aconitic acid was found to be significantly correlated with inflammatory response in an animal study[31]. The pathogenesis of NAFLD metabolism has been reported to be accompanied by these functional and phenotypic changes in liver pro-inflammatory macrophages. Pro-inflammatory M1 macrophages rely primarily on glycolysis and experience disruption in the mitochondrial TCA cycle, leading to the accumulation of itaconic acid, cis-Aconitic acid, and succinic acid[32]. Upregulation of glycolysis and disruption of the TCA cycle underpin this switch to activated liver pro-inflammatory macrophages. Moreover, excess cis-Aconitic acid may lead to the accumulation of HIF1α and activate the transcription of glycolytic genes, thus sustaining the glycolytic metabolism of liver pro-inflammatory M1 macrophages[32,33]. Our findings also indicated that cis-Aconitic acid was associated with impaired inflammation (IL1β, IL6, IL21, IL12, TNFα and CXCL8) and glycolipid metabolism.

Ribonolactone belongs to the class of carbohydrates, peptides, and analogues, and is mainly involved in the carbohydrate metabolism pathway. In the machine learning model, Ribonolactone showed good ability to discriminate the NASH patients from the controls. Recent evidence suggests that carbohydrate metabolism and TCA cycle metabolic pathway may be closely combined to play a synergistic role in the pathogenesis of NAFLD[32,34]. Specifically, concerning carbohydrate metabolism, glucose of amino acids, lactate, or glycerol is produced by glycogenolysis or gluconeogenesis, and De novo lipogenesis (DNL) is stimulated by carbohydrate and Acetyl-CoA[35]. Amino acid metabolism and carbohydrate metabolism are connected through the key metabolite pyruvate and participate in the progression of NAFLD through TCA cycle, a key signal pathway[32,34]. TCA cycle intermediates (Acetyl-CoA and Succinyl-CoA) are also involved in the progression of NAFLD[34,36].

This study identified three novel elevated inflammatory pathogenic metabolites (2-Hydroxy-3-methylbutyric acid, Ribonolactone, and cis-Aconitic acid) and the relationship between increased inflammation (CXCL8, IL17, IL6 and TNFα), may be involved in TLR5/MYD88/NFκB pathway, as shown in Fig. 5C. Specifically, 2-Hydroxy-3-methylbutyric acid, Ribonolactone, and cis-Aconitic acid mediated TLR5 signaling induces MYD88/IRAK4/TRAF6 by TAB1/TAB2/TAK1, and activation of NFκB by IKKs complex, and promoted the secretion of IL6 and TNFα[37,38].

Indole belongs to the class of aromatic heterocyclic organic compound, and is mainly involved in amino acid metabolism pathway. In the machine learning model, indole showed good ability in discriminating NASH patients from the controls. Indole and its derivatives have been indicated to have beneficial effects in mitigating liver inflammatory responses and preserving tight junctions of epithelial integrity[7,39]. An animal study showed that mice receiving indole displayed resistance to metabolic alternations of cholesterol and liver inflammation induced by lipopolysaccharide[40]. Some evidence also suggests that a certain dose of indole and its derivatives exert a protective effect, as it reduces the induction of pro-inflammatory cytokines including MCP-1, TNFα, and IL1β; and indole and its derivatives can be stimulated by ligand for pregnane X receptor and toll-like receptor 4 to act on both macrophages and hepatocytes against NAFLD[41,42]. These findings are consistent with our finding that the level of indole was significantly downregulated in NAFLD patients and associated with the effect of anti-inflammation (IL1β, IL6, IL17, TNFα, and CXCL8). The increase in indole-3-lactic acid consumes indole, leading to pro-inflammatory effects (IL1β, IL6, IL17, and IL21).

Collectively, our results capture a specific gut metabolite fingerprints in the clinical course of the NAFLD, and these metabolic reprogramming may provide potential insights and drivers into the pathogenesis of NAFLD in children. Pathway analysis of these differential gut metabolites in children with NAFLD demonstrated significant enrichment of several processes including amino acid metabolism, carbohydrate metabolism, digestive system, TCA cycle, energy metabolism and metabolism of cofactors and vitamins. These pathways have been reported to contribute to oxidative stress and systemic inflammation, which further lead to disorder in liver function and glycolipid metabolism[15,43,44]. The binding coefficients of the docking of metabolites to the ligand-binding regions of inflammatory receptors has the following practical significance. Firstly, by combining spatial and energy matching, the interaction force between inflammatory receptors and metabolites was qualitatively represented by the coefficient S value. When the S value is close to 0, it indicates that metabolite was unstable in combination with inflammatory receptor. In that case, this pair of inflammatory receptor and metabolite will not be considered for future in vitro experiments. This will greatly enhance the true positive rate of in vitro animal experiments, and optimize the efficiency of the use of research funds, especially when there are many metabolites that need to be

screened. The S value of the six receptors and metabolites in this study were all < −4 kcal/mol, indicating that metabolites were unstable in combination with inflammatory receptors in this study. Secondly, the smaller the binding coefficient S value, the more stable the conformation, indicating a stronger binding between the receptor and the metabolite. In the future vitro experimental validation, we will prioritize selecting pair of inflammatory receptor and metabolite with lower binding coefficients S value for animal experiments, such as pair of TLR5 and cis-Aconitic acid, pair of MyD88 and cis-Aconitic acid, and pair of TLR5 and 2-Hydroxy-3-methylbutyric acid, et al.

This study has a few limitations. First, some confounding factors, such as dietary habit and ethnicity, may influence the gut microbiota and metabolomic profiles. Second, although we successfully recruited 145 patients, the relatively small sample size may limit the generalizability and statistical significance of the results. However, high consistency of the gut and blood circulation results consolidated our findings. Future multicenter studies should consider expanding the sample size to enhance the robustness and external validity of these findings. Third, our study may not reflect changes in liver metabolites due to the poor accessibility of liver biopsy. Future studies in patients with liver biopsy are needed. Fourth, samples from the case cohort were collected after diagnosis of NAFLD, although most of them were collected closer to the date of diagnosis. Future studies of metabolomic profiles from more time points are required to explore molecular dynamics during temporal analysis of NAFLD progression. Finally, the investigation into the underlying mechanisms is still in its early stages. Future studies of in-depth in vitro experiments can better elucidate these mechanisms are needed, such as through the knockout or overexpression of TLR5 signaling pathway genes. Moreover, future studies need to consider incorporating animal or liver organoid model studies, which would greatly enhance the credibility and scientific rigor of the findings. This combined approach would provide a solid foundation for future drug development and clinical application.

We identified 9 metabolites that played a key role in metabolic reprogramming of lipids, carbohydrates, amino acid metabolism and TCA cycle, hence signifying their critical role in the inflammation pathogenesis of NAFLD, especially NASH. Machine learning analysis found that 7 metabolites play an important role in identifying disease states and verified by cell experiments in vitro and molecular-docking analysis. Last, this study identified three novel elevated inflammatory pathogenic metabolites (2-Hydroxy-3-methylbutyric acid, Ribonolactone, and cis-Aconitic acid) and the relationship between increased inflammation (CXCL8, IL17, IL6, and TNFα), may be involved in TLR5/MYD88/NFκB pathway.

Methods

Study population

This study was performed in 290 fecal samples and 290 plasma samples from 92 children with NAFLD (53 NAFL patients and 39 NASH patients) and 53 control children from the Institute of Child Health, Hunan children's Hospital (Changsha, China). All legal guardians of these children and the Hospital Ethics Research Committee (XYGW-2018-04) gave informed and written consent to the clinical and biomaterial omics investigations. The study was undertaken according to Helsinki Declaration II from January 2020 to September 2021. We recruited children with/without NAFLD with strict inclusion and exclusion criteria to avoid the influence on the targeted metabolites. A detailed selection flow chart of the children with/without NAFLD included in this study is shown in Fig. 6. According to the standard of "Screening for overweight and obesity among school-age children and adolescents" (WS/T 586-2018), the BMI status of children was classified into 3 categories, normal, overweight and obesity (Supplementary Table 11). Demographic, clinical data and inflammatory factors for each child were obtained at the Institute of Child Health, Hunan children's Hospital.

Analysis of gut metabolites by targeted metabolomics

Fecal and plasma levels of gut metabolites were determined by G350 Kit, measured using the liquid chromatography coupled to tandem mass spectrometry (LC-MS/MS). The G350 Kit has coverage of up to 346 metabolites and 40 biochemical classes, including the differential metabolites detected by our research group using untargeted screening and key metabolic pathways involved in the pathogenesis of NAFLD such as fatty acids, amino acids, and carbohydrates, as well as other metabolites such as indoles, bile acids and benzenoids[45–47]. Common nomenclature and biochemical classes of these gut metabolites are detailed in Supplementary Table 12.

Metabolite extractions

To extract metabolites from the fecal samples, 800 μL of cold methanol/acetonitrile/water (2:2:1) extraction solvent was added to 100 mg fecal sample, and adequately vortexed. Moreover, to extract metabolites from plasma samples, 400 μL of cold methanol/acetonitrile (1:1, v/v) extraction solvent was added to 100 μL plasma sample remove the protein and extract the metabolites, then adequately vortexed. For absolute quantification of the metabolites, stock solutions of stable- isotope internal standards were added to the extraction solvent simultaneously, and then the elution was collected and dried in a vacuum centrifuge at 4 °C. For LC-MS analysis, the samples were re-dissolved in 100 μL acetonitrile/water (1:1) solvent and transferred to LC vials.

LC-MS/MS analysis

Analyses were performed using an UHPLC (1290 Infinity LC, Agilent Technologies, USA) coupled to a QTRAP MS (6500, Sciex, USA). The analytes were separated on HILIC (Waters UPLC BEH Amide column, 2.1 mm × 100 mm, 1.7 μm) and C18 columns (Waters UPLC BEH C18-2.1 × 100 mm, 1.7 μm). For HILIC separation, the column temperature was set at 35 °C; and the injection volume was 2 μL. Mobile phase A: 100 mM ammonium acetate and 1.2% Ammonium hydroxide in water, mobile phase B: acetonitrile. A gradient (85% B at 0–1 min, 80% B at 3–4 min, 70% B at 6 min, 50% B at 10–12.5 min, 85% B at 12.6–18 min) was then initiated at a flow rate of 300 μL/min. For RPLC separation, the column temperature was set at 40 °C, and the injection volume was 2 μL. Mobile phase A: 50 mM ammonium formate and 0.4% formic acid in water, mobile phase B: methanol. A gradient (5% B at 0 min, 60% B at 5 min, 100% B at 11–13 min, 5% B at 13.1–16 min) was then initiated at a flow rate of 400 μL/min. The sample was placed at 4 °C during the whole analysis process. 6500 QTRAP (AB SCIEX, USA) was performed in positive and negative switch mode. The ESI positive source conditions were as follows: source temperature: 550 °C; ion Source Gas1 (Gas1): 55; Ion Source Gas2 (Gas2): 55; Curtain gas (CUR): 40; ion Sapary Voltage Floating (ISVF): +4500 V; the ESI negative source conditions were as follows: source temperature: 550 °C; Gas1: 55; Gas2: 55; CUR: 40; ISVF: −4500 V. MRM method was used for mass spectrometry quantitative data acquisition. A polled quality control (QC) samples were set in the sample queue to evaluate the stability and repeatability of the system. MultiQuant (version 3.0) was used for quantitative data processing. The ratio of the peak area (area of the peak for substance/area of the peak of the internal standard) was used for obtaining the absolute quantitation for each substance according to the calibration curve. Peakview (version 1.2) was used for the metabolomic total ion chromatograms (TIC) analysis of feces and plasma.

Cell lines

Human normal hepatocyte cell line hepatocytes (THLE-3) were obtained from the American Type Culture Collection (Manassas, Virginia, USA), which is non-tumorigenic and alpha fetoprotein expression negative. The cells were cultured in RPMI-1640 medium (GE Health Life Sciences, USA) supplemented with 10% (vol/ vol) fetal bovine serum (FBS) (Gibco, USA), and 1% penicillin/streptomycin (100 IU/ml penicillin and 100 mg/ml streptomycin) (Gibco, USA) at 37 °C in a humidified atmosphere of 5% CO^2. We terminated with 0.25% trypsin-EDTA (Gibco, USA) and collected logarithm growth cells. One million of THLE-3 was seeded in each well of a six-well culture plates. Then, cells were exposed to with or without indicated metabolites-supplemented for 24 h.

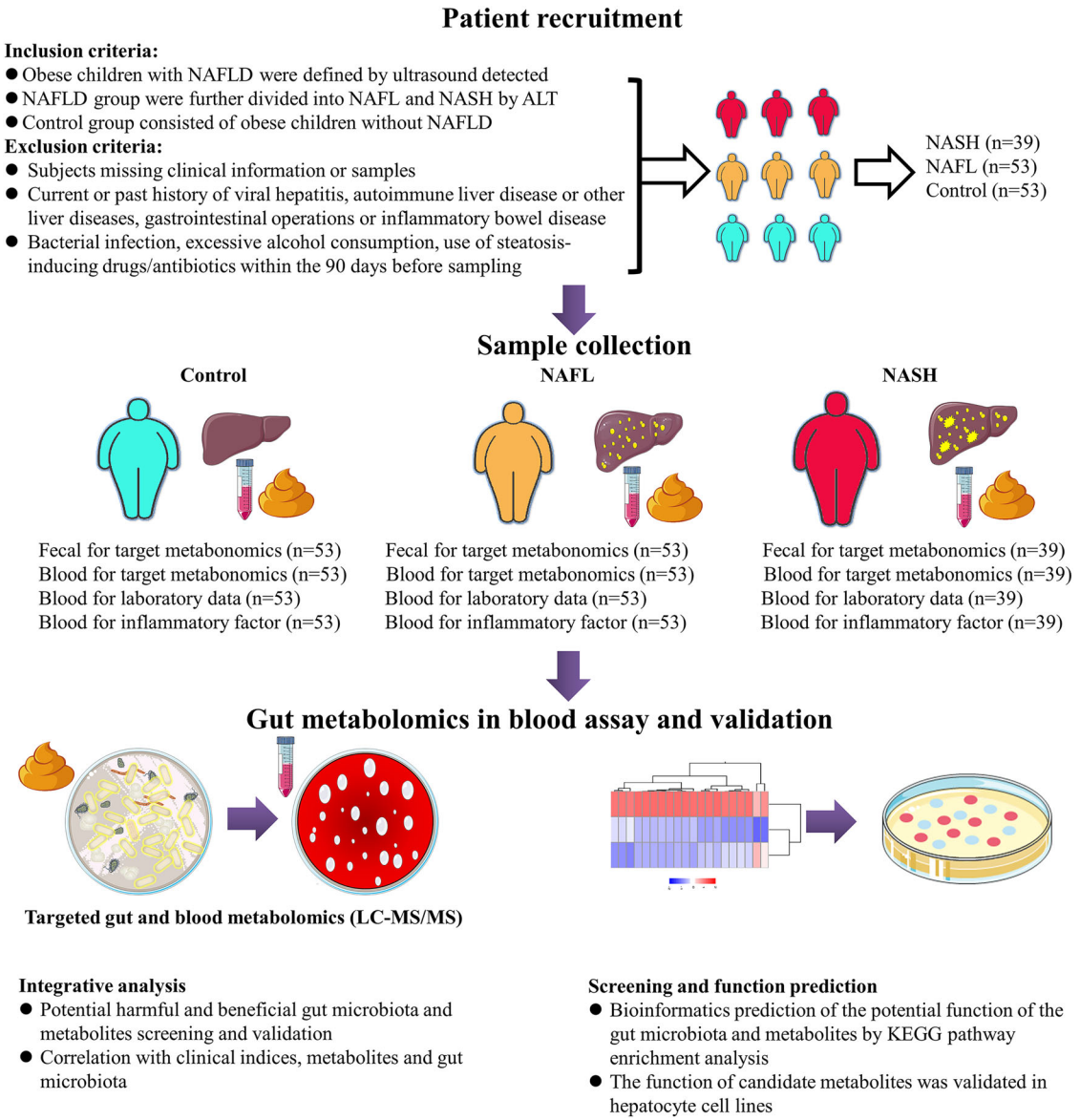

Fig. 6 | Flow chart showing the methods used for metabolomics analysis and bioinformatics function prediction. Patient recruitment and inclusion and exclusion criteria. Various clinical samples were obtained from NAFLD patients and controls. Integrative analysis for potential harmful and beneficial gut metabolites. Targeted metabolomics (LC-MS/MS) offers a plethora of information on metabolites. NAFL, nonalcoholic fatty liver, NASH non-alcoholic steatohepatitis, LC-MS/MS liquid chromatography coupled to tandem mass spectrometry, RF random forest.

Quantitative RT-PCR (qRT-PCR) for liver function and inflammation assay

Total cellular RNA was extracted using the RNA isolater Total RNA Extraction Reagent Kit (Vazyme, NanJing, China). Reverse transcription was conducted using the HiScript ® II Q Select RT SuperMix cDNA Synthesis Kit (Vazyme, NanJing, China) on S1000TM Thermal Cycler (Bio-Rad, Hercules, CA, USA). mRNAs were assayed qualitatively by ChamQ Universal SYBR qPCR Master Mix (Vazyme, NanJing, China) on a LightCycler96 Real-Time PCR System (Roche, Switzerland). All the procedures were repeated three times. The mRNA relative expression levels were calculated by the $2^{-\Delta\Delta Ct}$ method using GAPDH as an internal reference, respectively. The sequences of mRNA primer pairs used were in Supplementary Table 13.

Molecular docking of metabolites to binding domain of inflammatory receptor protein

The DOCK module of the MOE2019.01 software program was used to predict the preferable binding sites between inflammatory receptor and the respective metabolites. Water molecules in the crystal structure were removed with the MOE software, and the energy was minimized before molecular docking. The S value scoring function was based on GBVI/WSAΔG, that estimates the binding free energy of a metabolites to an inflammatory receptor.

Statistical analysis

All statistical tests were performed using R v3.5.1 statistical software. Non-parametric statistical tests (Kruskal-Wallis test/Mann–Whitney test) were used to assess the differences of demographic and clinical features between cases and controls. Spearman correlation was used to assess correlation between demographic and clinical features and gut metabolites. The hierarchical cluster analysis was used to assess clustering algorithm, and the Euclidean distance was used to assess the relationship between samples and gut metabolites; and between demographic and clinical features.

Data of gut metabolites were log transformed and centered before conducting the Orthogonal Partial least squares discriminant analysis

(OPLS-DA), which was used to assess the metabolic alterations between cases and controls. The Bonferroni correction was applied to correct for multiple-testing. The 7-fold cross-validation and 200 times permutation testing were used to assess the risk of overfitting and the robustness of the OPLS-DA model. The functions of differential metabolites were performed using the Kyoto Encyclopaedia of Genes and Genomes (KEGG) database.

Machine learning with random forest models was used to verify whether the metabolite combinations were potential discriminators for identifying children with NAFL or NASH. We selected important metabolites with mean decrease accuracy using RF analysis. Combined with important variables of machine learning screening, multivariate logistic regression analysis was used to control confounding factors such as age, BMI, and gender, and further account for the impact of these plasma metabolites on the children with NAFL or NASH. We further combined the results of RF analysis and biological function annotation to select potential inflammatory metabolites for the next in vitro cell experiment verification. Unless otherwise stated, $p < 0.05$ was considered statistically significant. Completed reporting checklist is shown in Supplementary Table 14.

Data availability

No datasets were generated or analysed during the current study.

Received: 9 September 2024; Accepted: 15 April 2025;
Published online: 01 July 2025

References

1. Brunt, E. M. et al. Nonalcoholic fatty liver disease. *Nat. Rev. Dis. Prim.* **1**, 15080 (2015).
2. Zhang, X. et al. Increasing prevalence of NAFLD/NASH among children, adolescents and young adults from 1990 to 2017: a population-based observational study. *BMJ Open* **11**, e042843 (2021).
3. Musso, G., Gambino, R. & Cassader, M. Non-alcoholic fatty liver disease from pathogenesis to management: an update. *Obes. Rev.***11**, 430–445 (2010).
4. Masoodi, M. et al. Metabolomics and lipidomics in NAFLD: biomarkers and non-invasive diagnostic tests. *Nat. Rev. Gastroenterol. Hepatol.* **18**, 835–856 (2021).
5. Aron-Wisnewsky, J., Warmbrunn, M. V., Nieuwdorp, M. & Clément, K. Nonalcoholic fatty liver disease: modulating gut microbiota to improve severity?. *Gastroenterology* **158**, 1881–1898 (2020).
6. Sztolsztener, K., Chabowski, A., Harasim-Symbor, E., Bielawiec, P. & Konstantynowicz-Nowicka, K. Arachidonic acid as an early indicator of inflammation during non-alcoholic fatty liver disease development. *Biomolecules* **10**, 1133 (2020).
7. Ma, L. et al. Indole alleviates diet-induced hepatic steatosis and inflammation in a manner involving myeloid cell 6-Phosphofructo-2-Kinase/Fructose-2,6-Biphosphatase 3. *Hepatology* **72**, 1191–1203 (2020).
8. Wang, X. et al. Contribution of endotoxin to Th17 bias in patients with non-alcoholic steatohepatitis. *Micro. Pathog.* **142**, 104009 (2020).
9. Cosentino, R. G. et al. Branched-chain amino acids and relationship with inflammation in youth with obesity: a randomized controlled intervention study. *J. Clin. Endocrinol. Metab.* **106**, 3129–3139 (2021).
10. Knudsen, C., Neyrinck, A. M., Lanthier, N. & Delzenne, N. M. Microbiota and nonalcoholic fatty liver disease: promising prospects for clinical interventions?. *Curr. Opin. Clin. Nutr. Metab. Care* **22**, 393–400 (2019).
11. Ali, M. H., Messiha, B. A. & Abdel-Latif, H. A. Protective effect of ursodeoxycholic acid, resveratrol, and N-acetylcysteine on nonalcoholic fatty liver disease in rats. *Pharm. Biol.* **54**, 1198–1208 (2016).
12. Ji, Y., Yin, Y., Li, Z. & Zhang, W. Gut microbiota-derived components and metabolites in the progression of non-alcoholic fatty liver disease (NAFLD). *Nutrients* **11**, 1712 (2019).
13. Liu, J. et al. Integrative metabolomic characterisation identifies altered portal vein serum metabolome contributing to human hepatocellular carcinoma. *Gut* **71**, 1203–1213 (2022).
14. Garcia, B. et al. Effects of branched-chain amino acids on the inflammatory response induced by LPS in Caco-2 Cells. *Metabolites* **14**, 76 (2024).
15. Lake, A. D. et al. Branched chain amino acid metabolism profiles in progressive human nonalcoholic fatty liver disease. *Amino Acids* **47**, 603–615 (2015).
16. Westerbacka, J. et al. Splanchnic balance of free fatty acids, endocannabinoids, and lipids in subjects with nonalcoholic fatty liver disease. *Gastroenterology* **139**, 1961–1971.e1961 (2010).
17. Misheva, M., Johnson, J. & McCullagh, J. Role of oxylipins in the inflammatory-related diseases NAFLD, obesity, and Type 2 diabetes. *Metabolites* **12**, 1238 (2022).
18. Ferrer, M. D. et al. Polyunsaturated and saturated oxylipin plasma levels allow monitoring the non-alcoholic fatty liver disease progression to severe stages. *Antioxidants* **12**, 711 (2023).
19. Chen, J. & Vitetta, L. Gut Microbiota metabolites in NAFLD Pathogenesis and therapeutic implications. *Int. J. Mol. Sci.* **21**, 5214 (2020).
20. Bing, H. & Li, Y. L. The role of bile acid metabolism in the occurrence and development of NAFLD. *Front. Mol. Biosci.* **9**, 1089359 (2022).
21. Sunny, N. E., Parks, E. J., Browning, J. D. & Burgess, S. C. Excessive hepatic mitochondrial TCA cycle and gluconeogenesis in humans with nonalcoholic fatty liver disease. *Cell Metab.* **14**, 804–810 (2011).
22. Sunny, N. E. et al. Cross-talk between branched-chain amino acids and hepatic mitochondria is compromised in nonalcoholic fatty liver disease. *Am. J. Physiol. Endocrinol. Metab.* **309**, E311–E319 (2015).
23. Ohie, T., Fu, X., Iga, M., Kimura, M. & Yamaguchi, S. Gas chromatography-mass spectrometry with tert.-butyldimethylsilyl derivation: use of the simplified sample preparations and the automated data system to screen for organic acidemias. *J. Chromatogr. B Biomed. Sci. Appl.* **746**, 63–73 (2000).
24. Walker, V. & Mills, G. A. Effects of birth asphyxia on urinary organic acid excretion. *Biol. Neonate* **61**, 162–172 (1992).
25. Zhou, B., Lou, B., Liu, J. & She, J. Serum metabolite profiles as potential biochemical markers in young adults with community-acquired pneumonia cured by moxifloxacin therapy. *Sci. Rep.* **10**, 4436 (2020).
26. Luukkonen, P. K. et al. Distinct contributions of metabolic dysfunction and genetic risk factors in the pathogenesis of non-alcoholic fatty liver disease. *J. Hepatol.* **76**, 526–535 (2022).
27. Li, M., Cai, S. Y. & Boyer, J. L. Mechanisms of bile acid mediated inflammation in the liver. *Mol. Asp. Med.* **56**, 45–53 (2017).
28. Ferslew, B. C. et al. Altered bile acid metabolome in patients with nonalcoholic steatohepatitis. *Dig. Dis. Sci.* **60**, 3318–3328 (2015).
29. Jian, H. et al. Amino acid and fatty acid metabolism disorders trigger oxidative stress and inflammatory response in excessive dietary valine-induced NAFLD of Laying Hens. *Front. Nutr.* **9**, 849767 (2022).
30. Cook, J. J. et al. Endurance exercise-mediated metabolic reshuffle attenuates high-caloric diet-induced non-alcoholic fatty liver disease. *Ann. Hepatol.* **27**, 100709 (2022).
31. Yu, F. et al. Exploring the metabolic phenotypes associated with different host inflammation of acute respiratory distress syndrome (ARDS) from lung metabolomics in mice. *Rapid Commun. Mass Spectrom.* **35**, e8971 (2021).
32. Viola, A., Munari, F., Sánchez-Rodríguez, R., Scolaro, T. & Castegna, A. The metabolic signature of macrophage responses. *Front. Immunol.* **10**, 1462 (2019).
33. Bailey, J. D. et al. Nitric oxide modulates metabolic remodeling in inflammatory macrophages through TCA cycle regulation and itaconate accumulation. *Cell Rep.* **28**, 218–230.e217 (2019).
34. Muyyarikkandy, M. S. et al. Branched chain amino acids and carbohydrate restriction exacerbate ketogenesis and hepatic

mitochondrial oxidative dysfunction during NAFLD. *Faseb J.* **34**, 14832–14849 (2020).
35. Goedeke, L. et al. Acetyl-CoA carboxylase inhibition reverses NAFLD and hepatic insulin resistance but promotes hypertriglyceridemia in rodents. *Hepatology* **68**, 2197–2211 (2018).
36. Fletcher, J. A. et al. Impaired ketogenesis and increased acetyl-CoA oxidation promote hyperglycemia in human fatty liver. *JCI insight* **4**, e127737 (2019).
37. Huang, J. et al. Effect of curcumin on regulatory B cells in chronic colitis mice involving TLR/MyD88 signaling pathway. *Phytother. Res.* **37**, 731–742 (2022).
38. Tallant, T. et al. Flagellin acting via TLR5 is the major activator of key signaling pathways leading to NF-kappa B and proinflammatory gene program activation in intestinal epithelial cells. *BMC Microbiol.* **4**, 33 (2004).
39. Krishnan, S. et al. Gut Microbiota-Derived Tryptophan metabolites modulate inflammatory response in hepatocytes and macrophages. *Cell Rep.* **23**, 1099–1111 (2018).
40. Beaumont, M. et al. The gut microbiota metabolite indole alleviates liver inflammation in mice. *Faseb J.* **32**, fj201800544 (2018).
41. Natividad, J. M. et al. Impaired aryl hydrocarbon receptor ligand production by the gut microbiota is a key factor in metabolic syndrome. *Cell Metab.* **28**, 737–749.e734 (2018).
42. Venkatesh, M. et al. Symbiotic bacterial metabolites regulate gastrointestinal barrier function via the xenobiotic sensor PXR and Toll-like receptor 4. *Immunity* **41**, 296–310 (2014).
43. Gaggini, M. et al. Altered amino acid concentrations in NAFLD: impact of obesity and insulin resistance. *Hepatology* **67**, 145–158 (2018).
44. Donnelly, K. L. et al. Sources of fatty acids stored in liver and secreted via lipoproteins in patients with nonalcoholic fatty liver disease. *J. Clin. Investig.* **115**, 1343–1351 (2005).
45. Bechmann, L. P. et al. Free fatty acids repress small heterodimer partner (SHP) activation and adiponectin counteracts bile acid-induced liver injury in superobese patients with nonalcoholic steatohepatitis. *Hepatology* **57**, 1394–1406 (2013).
46. Legry, V. et al. Bile acid alterations are associated with insulin resistance, but not with NASH, in Obese Subjects. *J. Clin. Endocrinol. Metab.* **102**, 3783–3794 (2017).
47. Haufe, S. et al. Branched-chain and aromatic amino acids, insulin resistance and liver specific ectopic fat storage in overweight to obese subjects. *Nutr. Metab. Cardiovasc. Dis.* **26**, 637–642 (2016).

Acknowledgements

The authors would like to thank Central South University Library for the literature search help. Furthermore, we sincerely appreciate the hard work of the distinguished editors and reviewers, which improved the clarity of this article. This work was supported by Hunan Provincial Natural Science Foundation of China (2024JJ6257), Opening fundings of Hunan Provincial Key Laboratory of Pediatric Orthopedics (2023TP1019), Science and Technology Project of Furong Laboratory (2023SK2111), Hunan Provincial Clinical Medical Research Center for pediatric Limb Deformities (2019SK4006).

Author contributions

X.P. and J.L. contributed to the study design, while X.L., H.Z., A.K., and J.L. contributed to the data collection. Statistical analyses and interpretation of results were performed by Y.Z., N.X., J.W., A.K., and M.L., whereas X.P., W.D., and J.L. drafted the manuscript and edited the language. All authors contributed to the article and approved the submitted version.

Competing interests

The authors declare no competing interests.

Additional information

Supplementary information The online version contains supplementary material available at https://doi.org/10.1038/s41522-025-00706-w.

Correspondence and requests for materials should be addressed to Xiongfeng Pan.